Organic & Biomolecular Chemistry

PAPER

View Article Online
View Journal | View Issue

Cite this: *Org. Biomol. Chem.*, 2017, **15**, 3603

Improving target amino acid selectivity in a permissive aminoacyl tRNA synthetase through counter-selection†

Itthipol Sungwienwong,‡[a] Zachary M. Hostetler,‡[b] Robert J. Blizzard,[c] Joseph J. Porter,[c] Camden M. Driggers,[d] Lea Z. Mbengi,[d] José A. Villegas,[a] Lee C. Speight,[a] Jeffery G. Saven,[a] John J. Perona,[d,e] Rahul M. Kohli,[b] Ryan A. Mehl[c] and E. James Petersson *[a]

Received 8th March 2017,
Accepted 3rd April 2017

DOI: 10.1039/c7ob00582b

rsc.li/obc

The amino acid acridon-2-ylalanine (Acd) can be a valuable probe of protein dynamics, either alone or as part of a Förster resonance energy transfer (FRET) or photo-induced electron transfer (eT) probe pair. We have previously reported the genetic incorporation of Acd by an aminoacyl tRNA synthetase (RS). However, this RS, developed from a library of permissive RSs, also incorporates *N*-phenyl-aminophenyl-alanine (Npf), a trace byproduct of one Acd synthetic route. We have performed negative selections in the presence of Npf and analyzed the selectivity of the resulting AcdRSs by *in vivo* protein expression and detailed kinetic analyses of the purified RSs. We find that selection conferred a ~50-fold increase in selectivity for Acd over Npf, eliminating incorporation of Npf contaminants, and allowing one to use a high yielding Acd synthetic route for improved overall expression of Acd-containing proteins. More generally, our report also provides a cautionary tale on the use of permissive RSs, as well as a strategy for improving selectivity for the target amino acid.

Introduction

It is now well-established that protein folding and dynamics play essential roles in health and disease. For example, the small protein calmodulin (CaM) undergoes a dramatic conformational rearrangement to carry out its calcium sensor function in eukaryotic cells.[1,2] In a second example, the bacterial repressor-protease LexA uses a complex sequence of RecA-induced structural change, self-proteolysis, and dissociation of subunits to sense DNA damage and activate genes that ultimately lead to antibiotic resistance.[3,4] Finally, the conformational flexibility of the neuronal protein α-synuclein (αS) is a liability, as it leads αS to misfold and form amyloid fibrils that contribute to the pathogenesis of Parkinson's disease.[5,6] Fluorescence spectroscopy is a powerful tool for studying such processes, as it allows one to observe protein motions in real time under physiological conditions, including measurements in live cells.[7,8] One can even obtain low resolution structural information using distance-dependent chromophore interactions such as Förster resonance energy transfer (FRET) and quenching by photo-induced electron transfer (eT).[9] To appropriately model protein motions, one needs a set of probes that are capable of accurately reporting on distance changes without disrupting the fold and function of the protein of interest.[10]

Recent developments in genetic code expansion and bioorthogonal chemistry have made the site-specific incorporation of non-canonical amino acids (ncAAs) and installation of fluorophores through post-translational modification straightforward, even in cells or lysates.[11] Unfortunately, the fluorophores used in these approaches are often relatively large and are attached by long flexible linkers, which have a non-trivial impact on the observed FRET measurements. Additionally, larger fluorophores cannot be introduced co-translationally to allow packing into the interior of a folded protein. Thus, they

[a]*Department of Chemistry, University of Pennsylvania, 213 South 34th Street, Philadelphia, PA 19104, USA. E-mail: ejpetersson@sas.upenn.edu; Tel: +1-215-746-2221*
[b]*Department of Medicine, Perelman School of Medicine, University of Pennsylvania, 3610 Hamilton Walk, Philadelphia, PA 19104, USA*
[c]*Oregon State University, Department of Biochemistry and Biophysics, 2011 Ag Life Sciences Building, Corvallis, Oregon 97331, USA*
[d]*Department of Chemistry, Portland State University, P.O. Box 751, Portland, Oregon 97207, USA*
[e]*Department of Biochemistry & Molecular Biology, Oregon Health & Sciences University, 3181 Southwest Sam Jackson Park Road, Portland, Oregon 97239, USA*

†Electronic supplementary information (ESI) available: Procedures for the expression and characterization of proteins, analysis of enzyme kinetics, and structural modeling. See DOI: 10.1039/c7ob00582b

‡These authors contributed equally to this work.

will be restricted to surface-accessible positions, limiting the regions of the protein for which conformational changes can be studied.

Smaller probes that are more closely tied to the backbone are better able to report on conformational changes of the protein. The Petersson laboratory has developed small fluorescent probes and quenchers that should be non-perturbing to proteins and which are closely tied to the protein backbone. These include thioamide substitutions of the backbone itself and intrinsically fluorescent ncAAs such as acridon-2-ylalanine (Acd or **1**).[12] These new approaches are significant because, of the >100 ncAAs that have been genetically encoded in *E. coli*, only four are fluorescent.[12–19]

Acd is a blue-wavelength fluorescent amino acid that is a useful fluorophore because of its small size (222 Å^3), near unity quantum yield in water (ϕ = 0.95), unusually long lifetime ($\tau \sim 15$ ns) and high photostability (<5% degradation after 3 h irradiation).[20–22] Previous work in the Petersson laboratory has shown that Acd can be efficiently quenched by a thioamide through an eT mechanism.[23] We have also shown that it can be a valuable intermolecular FRET acceptor from Trp or methoxycoumarin (Mcm), and a donor to more red-shifted dyes such as nitrobenzoxadiazole (NBD) or fluorescein.[12] Further examples of the utility of Acd in intramolecular FRET with Mcm and in fluorescence polarization studies of protein binding are shown in Fig. S8 and S9 (see ESI†).

Previously, the Mehl and Petersson laboratories developed an *in vivo* system for Acd incorporation using methods pioneered by Schultz.[24] These methods require the generation of an aminoacyl tRNA synthetase (RS) that is selective for the ncAA and a tRNA that can be selectively charged by the ncAARS to deliver the tRNA to an unassigned codon, typically the amber stop codon UAG (tRNA$_{CUA}$).[25] An RS was selected from a library of permissive *M. janaschii* (*Mj*) tyrosyl RS mutants that had previously been shown to incorporate bulky aromatic amino acids such as 4-(2′-bromoisobutyramido) phenylalanine (Brb) and *p*-benzoyl phenylalanine.[26–28] The most active mutant from this library (G2) was used to express Acd-containing variants of CaM, triose phosphate isomerase, and αS.[12] Here, we will refer to this mutant as AcdRS1.

At the same time, we also developed an efficient synthetic route, starting from the natural amino acid Tyr (**2**) and using a Buchwald–Hartwig coupling to *O*-methyl anthranilate (**4**) to form **5** (see Scheme 1).[12] We obtained an 86% overall yield from Tyr using the route shown in Scheme 1 with H_2SO_4 used in the Friedel–Crafts cyclization step (no racemization observed by high performance liquid chromatography, HPLC). Unfortunately, this route also produced a decarbonylated byproduct, *N*-phenyl-aminophenyl alanine (Npf or **6**) in trace amounts. We found that Npf was in fact incorporated much more efficiently by AcdRS1 than Acd. We were able to initially address this problem by converting **5** to Acd using LiOH deprotection followed by PPA cyclization. This eliminated Npf formation, but limited us to a 44% overall yield from Tyr with complete racemization (a 22% yield of the requisite L-Acd form). While we were able to express proteins containing exclusively Acd, this was not a very satisfactory solution, and we sought to obtain an AcdRS that was sufficiently selective against Npf that we could use the higher yielding H_2SO_4 synthetic route.

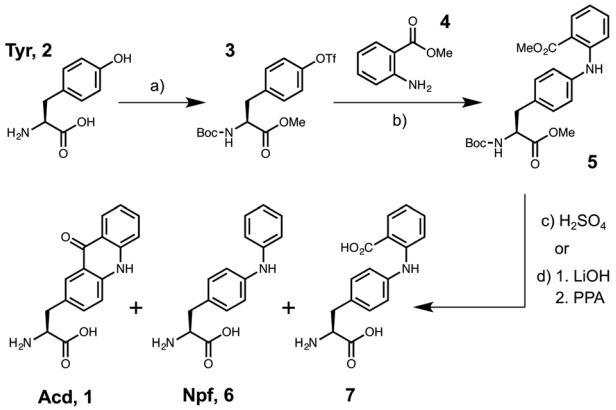

Scheme 1 Synthesis of Acd by H_2SO_4 or polyphosphoric acid (PPA) routes. (a) 1. $SOCl_2$, MeOH 2. Boc_2O, Na_2CO_3, THF/H_2O (3 : 1) 3. $PhNTf_2$, DMAP, NEt_3, CH_2Cl_2; 88% yield over 3 steps; (b) $Pd(OAc)_2$, *rac*-BINAP, Cs_2CO_3; 92% yield; (c) H_2SO_4, reflux; 98% yield; (d) 1. LiOH, 2. PPA; 53% yield over two steps (racemic mixture).

A typical selection experiment to evolve RSs for ncAAs consists of rounds of positive selection (performed in the presence of the ncAA and the 20 canonical amino acids) and negative selection (performed in the presence of only the 20 canonical amino acids). In this work, we sought to obtain an Acd-selective RS by performing these standard selections, as well as negative selections where Npf was included in the selection media to eliminate those AcdRS mutants charging tRNA with Npf. This resulted in two additional RSs, AcdRS2a (clone G11, from traditional negative selection) and AcdRS2b (clone A9, from Npf counter-selection), which both showed good selectivity in an initial screen in which the ncAAs were incorporated into green fluorescent protein (GFP).

We have performed detailed studies of their *in vivo* selectivities in expressions of CaM, αS, and LexA and found that AcdRS2b has superior selectivity for Acd when compared to AcdRS2a. We have also expressed and purified AcdRS1 and AcdRS2b to measure their Acd and Npf activation kinetics. We are able to rationalize their selectivities in terms of the X-ray crystal structure of AcdRS1 and a homology model of AcdRS2b. Our study provides an improved Acd incorporation method for fluorescent labeling of proteins, and it also validates a general strategy for how one may optimize a permissive RS to eliminate incorporation of an unwanted contaminant.

Results and discussion

CaM, LexA and αS constructs with TAG mutations were expressed in *E. coli* along with plasmids encoding AcdRS1 and its cognate tRNA$_{CUA}$ species. We analyzed the selectivity of AcdRS1 based on matrix-assisted laser desorption ionization

(MALDI) mass spectrometry (MS) data of both intact and trypsin-digested purified proteins, including CaM, LexA, and αS. Data for incorporation at position 113 in CaM are shown in Fig. 2 and 3; additional data for LexA and αS are shown in the ESI.† In all cases, when the proteins are expressed using media containing pure Npf or Acd produced using the PPA route, a single peak for the intended product is obtained in the MALDI spectra. When the proteins are expressed in media containing Acd produced using the H_2SO_4 route, we observe a roughly 45 : 55 Npf/Acd ratio of the two CaM species, even though Npf is present only in trace quantities. We also considered the possibility that Npf could be generated *in vivo* by several possible routes. For example, a carboxy-lyase such as YigC could convert 7 (also a <1% contaminant in the H_2SO_4 Acd synthesis) into Npf,[29] or some fraction of Acd could be converted to Npf. Our PPA Acd expression data allow us to exclude metabolic processing of Acd, since we see no Npf incorporation in this case. When we use media in which we intentionally include 1% or 10% Npf with Acd, we detect products containing Npf/Acd ratios of 65 : 35 and >95 : 5, respectively (ESI, Fig. S2†). These data and similar data for other proteins (see ESI†) indicated to us that the selectivity of our nominal AcdRS—designed to incorporate Acd specifically—in fact favored Npf incorporation by approximately 100-fold. Despite the incongruity between its intended use and its actual fidelity, one should keep in mind that AcdRS1 was selected based on expression yields of GFP in the presence of media containing Acd from the H_2SO_4 route (and therefore containing ~1% Npf). Similar contamination, barely detectable by HPLC analysis, may be present in other stocks of home-synthesized or commercial batches of ncAAs used in RS selection.

AcdRS optimization

RS selection to remove Npf activity. To reduce the incorporation of Npf, we used a GFP expression screen common to the Mehl laboratory to screen mutant *Mj* TyrRS libraries with positions in the amino acid binding pocket randomized.[27,30] Two rounds of positive and negative selection were performed according to standard protocols, with the desired ncAA (*i.e.*, Acd) present in the media for rounds of positive selection and only the 20 canonical amino acids present in the media for rounds of negative selection. In parallel, we also performed a similar two round selection experiment with a novel negative selection step that included the undesired Npf in the media. Thus, in this second "counter-selection" protocol, we explicitly selected against Npf incorporation rather than relying on high activity for Acd to be mutually exclusive of activity for Npf. The *Mj* RS libraries were based around the G2 (AcdRS1) and F9 clones, both of which incorporate Acd, and have very similar sequences. The level of Npf misincorporation is noticeably higher for F9 than for G2, highlighting the idea that small sequence changes can have a large impact on selectivity.

From these two selection protocols, eleven RS clones were identified that showed high levels of Acd incorporation. Of these clones, only A9 derived from the Npf counter-selection. Among the ten clones from the standard negative selection, the G11 clone demonstrated the highest level of selectivity as measured by the GFP fluorescence of cell suspensions expressed in media containing either 1 mM Acd or 1 mM Npf (Fig. 1 and ESI Fig. S1†). Therefore, the G11 and A9 RSs were cloned into the pDule2 vector for expression of other proteins, and are referred to as AcdRS2a and AcdRS2b, respectively.

Comparison of AcdRS active sites. The availability of an X-ray crystal structure of AcdRS1 (G2) allowed us to examine the sequences of various library members to understand how changes might confer increased selectivity for Acd relative to Npf. Although we were never able to obtain suitably diffracting crystals of an Acd complex with AcdRS1, the Mehl group has previously published a structure of this RS with Brb bound (Fig. 1, Middle). Recall that "AcdRS1" is a permissive RS, as can be seen in an analysis of its activation of a variety of aromatic ncAAs in Cooley *et al.*[30] Brb, Npf, and Acd share the

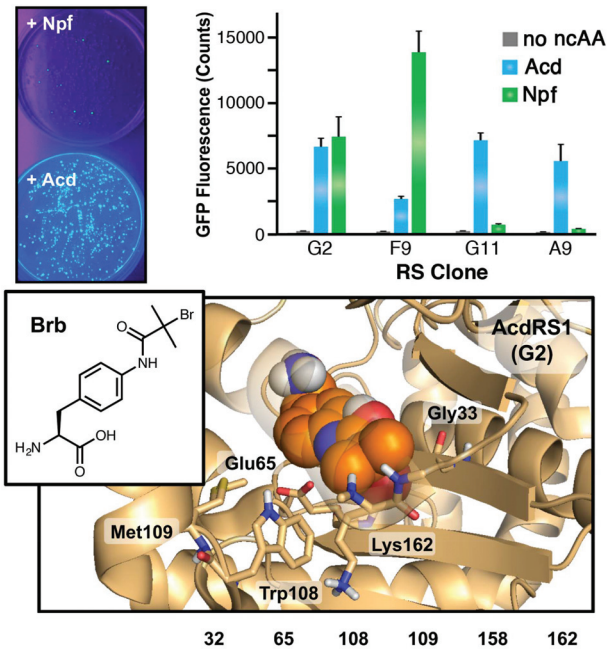

	32	65	108	109	158	162
Mj TyrRS	Tyr	Leu	Phe	Gln	Asp	Leu
AcdRS1 (G2)	Gly	Glu	Trp	Met	Ser	Lys
F9	Gly	Glu	Phe	Gln	Gly	Lys
AcdRS2a (G11)	Ala	Tyr	His	Glu	Ser	Ser
AcdRS2b (A9)	Ala	Asp	Leu	Glu	Ser	Thr

Fig. 1 AcdRS selection. Top Left: Images of *E. coli* agar plates used in rounds of positive (+ Acd) and negative (+ Npf) selection. Media for both plates also contain sources of the 20 canonical amino acids. Top Right: Fluorescence of suspensions of *E. coli* cells expressing GFP with a TAG codon at position 150 using the indicated RS clone and amino acid mixture. Emission was measured at 528 nm with excitation at 485 nm. Middle: Image of the AcdRS1 (G2) active site with radical polymerization initiator Brb bound (PDB ID: 4PBR). A favourable hydrogen bond between the carboxylate of Glu_{65} and the aniline N–H of Brb can be seen. Bottom Sequences of *Mj* RS clones used for incorporation of Acd. Additional sequences of clones from GFP-based screening are given in the ESI.†

feature of a nitrogen atom in the *para* position of the phenylalanine ring, which seems to be a key recognition determinant as it can hydrogen bond with Glu_{65}. Both of the RS clones that give the highest selectivity for Acd, AcdRS2a (G11) and AcdRS2b (A9), have a mutation at this position, but one that maintains the potential hydrogen bond acceptor functionality. Other library members with Pro, Trp, Ile, or Val at position 65 had less than ten-fold selectivity for Acd over Npf in the GFP assay (see ESI† for details). Further analysis of AcdRS1 (G2), AcdRS2a (G11), and AcdRS2b (A9) selectivity based on homology modelling and docking studies is given below.

Analysis of AcdRS selectivity

***In vivo* characterization of AcdRS selectivity.** To more rigorously investigate the selectivity of AcdRSs 2a and 2b, we expressed proteins in *E. coli*, purified them, and analyzed ncAA incorporation by MALDI MS of whole proteins and trypsin digests. As above, each experiment was carried out under five media conditions, varying in the amino acid provided and/or the synthetic route by which it was obtained: with H_2SO_4 Acd, PPA Acd, Npf, 1% Npf/Acd, and 10% Npf/Acd. Data for incorporation at position 113 in CaM are shown in Fig. 2 and 3; data for αS and LexA are shown in the ESI.† As anticipated from the GFP screening data, we found that both AcdRS2a and 2b have improved selectivity against Npf. However, AcdRS2a still gives a mixture of Npf- and Acd-containing protein when H_2SO_4 Acd is used in the growth media. In contrast, proteins expressed using AcdRS2b contain only Acd, even when challenged with 10% Npf in the media. This level of selectivity was observed in CaM, αS, and LexA (Fig. 2 and ESI Fig. S2–S4†). It should also be noted that AcdRS2b selectivity is observed in a variety of media. CaM and αS are expressed in minimal media or Luria broth (LB) with isopropyl β-D-1-thiogalactopyranoside (IPTG) induction, while LexA is expressed in richer, lactose auto-induction media. Based on these data, we selected the AcdRS2b (A9) for further characterization.

For a more rigorous, quantitative analysis of selectivity, we analyzed the CaM trypsin digest data by normalizing the intensity of the peak for the 108–116 fragment, containing Acd or Npf at position 113, to the intensity of the peak for the 117–127 fragment (Fig. 3). $CaM_{117–127}$ should be produced in a 1 : 1 ratio with $CaM_{108–116}$ when the protein is completely digested by trypsin, and this can be confirmed by varying the digest time and observing that the intensity ratios do not change (data not shown). Normalization using an internal standard is essential to interpreting the intensity data correctly. The $CaM_{108–116}Acd_{113}$ fragment (A in Fig. 3) ionizes 5.5-fold better than the $CaM_{117–127}$ fragment (* in Fig. 3), while the $CaM_{108–116}Npf_{113}$ fragment (N in Fig. 3) ionizes 6.1-fold

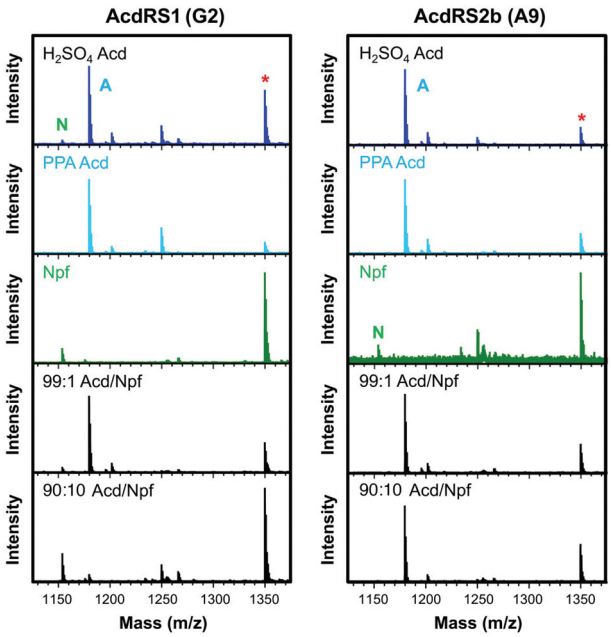

Fig. 3 CaM_{113} trypsin digest data for AcdRS selectivity analysis. CaM (UAG codon at 113) was expressed in minimal media containing 1 mM ncAA: Acd, synthesized either using the H_2SO_4 route or PPA route, Npf, or either a 99 : 1 or 90 : 10 mixture of PPA Acd and Npf. Expression was performed with one of the three AcdRSs indicated. The peaks for the $(M + H)^+$ masses of the $CaM_{108–116}Acd_{113}$ fragment (A, 1179.8 Da), $CaM_{108–116}Npf_{113}$ fragment (N, 1153.8 Da), and $CaM_{117–127}$ fragment (*, 1349.9 Da) are indicated. The intensities of the $CaM_{108–116}Acd_{113}$ and $CaM_{108–116}Npf_{113}$ fragment peaks were normalized using the intensity of the $CaM_{117–127}$ fragment peak.

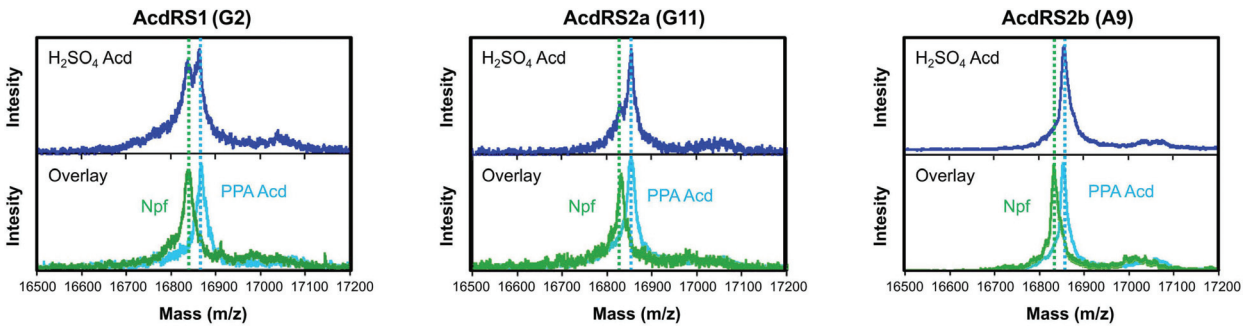

Fig. 2 *In Vivo* AcdRS Selectivity. CaM (UAG codon at 113) was expressed in minimal media containing 1 mM ncAA: Acd, synthesized either using the H_2SO_4 route or PPA route, or Npf. Expression was performed with one of the three AcdRSs indicated. Significant incorporation of Npf is seen for AcdRS2a (G11) when using H_2SO_4 Acd, but only Acd-containing protein is seen with AcdRS2b (A9). Experimental details are given in the ESI.†

worse than the $CaM_{117-127}$ fragment. This can be seen by examining the peak ratios for PPA Acd (*i.e.*, Acd only) and Npf expressions. After peak scaling, one obtains an MS-based Acd/Npf selectivity ratio (MS Sel) of 2.6×10^{-3} for AcdRS1 and 0.20 for AcdRS2b, calculated as follows:

$$\text{MS Sel} = (\text{Scaled Acd}/\text{Scaled Npf})/(\text{Acd}/\text{Npf ratio in media}).$$

The AcdRS1 MS Sel value is in good agreement with our estimate of 100-fold selectivity for Npf based on the less quantitative whole protein MALDI MS data. While the AcdRS2b MS Sel value may seem surprisingly low given the absence of any obvious $CaM_{108-116}Npf_{113}$ peak in the MALDI spectra, it is important to keep in mind that the RS is only being challenged with at most 10% Npf in the media and that $CaM_{108-116}Npf_{113}$ ionizes 30-fold worse than $CaM_{108-116}Acd_{113}$. Using these Acd/Npf selectivity ratios, we determined that selection resulted in a 76-fold improvement in selectivity for AcdRS2b relative to AcdRS1. We note that the effective *in vivo* Acd selectivities for both AcdRS1 and AcdRS2b are less than one and are probably influenced by preferential uptake of Npf into cells.

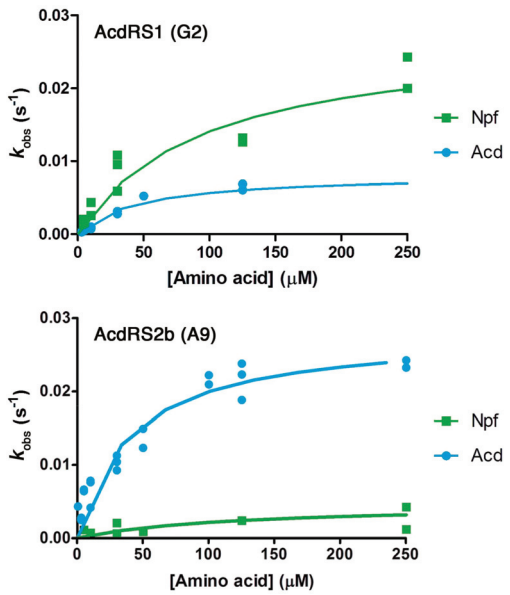

Fig. 4 tRNA Aminoacylation Kinetics. Plot of k_{obs} for reactions of AcdRS1 and AcdRS2b as a function of Acd or Npf concentration. Reaction rates were determined using thin layer chromatography following nuclease digestion of aminoacylated tRNA as described in the ESI.† Sample primary data are shown in Fig. S7.† Rate constants were determined from progress curves for each enzyme at varying amino acid concentrations.

***In Vitro* characterization of RS activity.** To better understand AcdRS1 and 2b selectivity, we generated His-tagged variants of the enzymes, then expressed and purified them for *in vitro* activity assays. Charging of tRNA by RSs is a two-step process, where the first step is the RS-catalyzed reaction of amino acid with ATP to form an aminoacyl-adenylate intermediate (Aa-AMP), releasing inorganic pyrophosphate (PP_i); and the second step is the reaction of this enzyme-bound adenylate with the the 2′ or 3′ hydroxyl group on A76 at the 3′ end of the tRNA.[31]

$$\text{Aa} + \text{ATP} \rightarrow \text{Aa-AMP} + PP_i \quad (1)$$

$$\text{Aa-AMP} + \text{tRNA} \rightarrow \text{Aa-tRNA} + \text{AMP} \quad (2)$$

While some prior studies have used assays that measure only the first step of the aminoacylation reaction to demonstrate that *in vitro* activities are consistent with ncAA incorporation,[24,32,33] it has been shown by the Perona laboratory that full tRNA aminoacylation assays correlate well with *in vivo* observations of RS activity.[34] This is expected, since amino acid incorporation into protein *in vivo* can only occur upon aminoacylation. Thus, aminoacylation of an *in vitro* transcribed ^{32}P-labeled $tRNA_{CUA}$ was measured under single-turnover conditions at a variety of Acd or Npf concentrations for AcdRS1 and AcdRS2b. Plots of the first-order rate constants as a function of amino acid concentration were used to determine k_{obs} and K_d for each amino acid and RS combination, as previously described.[35] (Fig. 4 and Table 1) For these measurements, k_{obs} corresponds to the microscopic rate constant for the chemical steps of aminoacylation, or to a closely linked first-order rearrangement that follows tRNA binding and precedes aminoacylation.

Comparative kinetic analysis of AcdRS1 and AcdRS2b reveals catalytic preferences that correlate well with measurements of amino acid incorporation *in vivo* and mass spectrometry of proteins incorporating Acd and Npf. AcdRS1 aminoacylates $tRNA_{CUA}$ with Acd three-fold slower than with Npf, while AcdRS2b aminoacylates $tRNA_{CUA}$ with Acd five-fold faster than with Npf (Table 1). These changes in k_{obs} are primarily responsible for the change in selectivity between the RSs, as there are only relatively minor differences in K_d for the ncAAs. The enzymological selectivity (Enz Sel), calculated as

$$\text{Enz Sel} = [k_{obs}(\text{Acd})/K_d(\text{Acd})]/[k_{obs}(\text{Npf})/K_d(\text{Npf})]$$

changes from about a two-fold Npf preference by AcdRS1 to 16-fold Acd selectivity for AcdRS2b. Overall, AcdRS2b is improved in selectivity for Acd relative to Npf by 34-fold, in reasonable agreement with the 76-fold specificity shift derived from the *in vivo* measurements made based on trypsin digest peak intensities. Note that while the relative change in selecti-

Table 1 AcdRS *in vitro* enzymology and *in vivo* MS selectivity parameters

AcdRS	k_{obs} (Acd) $\times 10^{-3}$ s^{-1}	K_d (Acd) μM	k_{obs} (Npf) $\times 10^{-3}$ s^{-1}	K_d (Npf) μM	Enz Sel	MS Sel
1 (G2)	8.0 ± 2.0	45.1 ± 18.8	24.0 ± 1.0	64.1 ± 10.8	0.47	2.6×10^{-3}
2b (A9)	28.0 ± 2.0	39.9 ± 6.8	5.0 ± 1.0	114 ± 10.0	16	0.20

vity is consistent between the *in vitro* and *in vivo* data, the actual selectivities are quite different, presumably because the *in vivo* MS Sel is the product of Enz Sel and factors affecting the availabilities of the amino acids inside the cells. We estimate that the effective Npf concentration in cells is about 100-fold greater than the Acd concentration. This could be the result of preferential uptake of Npf, or sequestration of Acd by binding to other targets. Such targets could include DNA or RNA, both of which are known targets of acridone-based intercalator molecules.[36] Thus, to prevent Npf misincorporation, AcdRS2b must be significantly Acd-selective, even though Npf contaminants are only present at about 1% (10 μM) in the media.

Modeling of AcdRSs complexed with Npf and Acd. To inform the differences in Acd and Npf charging activity, models were built based upon the crystallographic structure of AcdRS1 complexed with Brb (PDB ID: 4PBR).[30] In generating a model of AcdRS1 (G2), the phenyl ring on the Brb ligand guided the placement of Acd and Npf within the binding pocket (Fig. 5). Hydrogen atoms were added to the protein, and the ligand structure was energy minimized within the fixed protein structure. For Acd, a void volume remains between the molecule and the G_{32}–G_{34} β-strand. In each G2 complex, Glu_{65} is poised to accept a hydrogen-bond from the N–H of the ligand's side chain. For Npf, the additional free volume allows the molecule to relax to a twisted conformation, alleviating repulsive internal steric contacts between the ligand's two phenyl rings. Using the same protein structure, computational protein design methods developed in the Saven laboratory were used to generate a model of A9,[37–40] followed by energy minimization of the atomic coordinates of the ligands and the mutated side chains (Fig. 5). In A9, the $Gly_{32}Ala$ mutation forces Npf to adopt a more planar conformation of the ligand's two phenyl rings in order to form a hydrogen bond with Asp_{65}. Instead, Npf relaxes to avoid this high-energy distortion, which not only prevents hydrogen bonding of the Npf aniline N–H with Asp_{65}, but also forces the Asp_{65} sidechain to move. While it is possible that the actual conformations adopted in the active site are different in the presence of tRNA, these models are consistent with AcdRS2b's increased activity toward Acd relative to Npf. Thus, it appears that the combination of the $Gly_{32}Ala$ and $Glu_{65}Asp$ mutations provides the increase in Acd selectivity for AcdRS2b (A9). Further experimental studies of single point mutations are required to validate this hypothesis, and will be reported when complete.

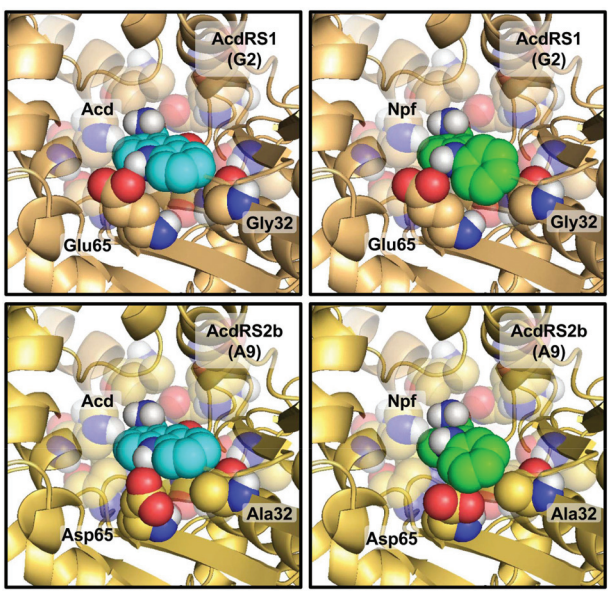

Fig. 5 AcdRS Homology Models. Acd or Npf were energy minimized in the active site of AcdRS1 (G2), taken directly from PDB structure file 4PBR, or a model of AcdRS2b (A9). Npf is accommodated in the AcdRS1 active site where the phenyl rings can become non-planar with respect to each other. In the A9 active site, Npf twisting is restricted by the Ala_{32} sidechain, and a hydrogen bond cannot be made with Asp_{65}.

Conclusions

Our elucidation of the process by which trace Npf in the Acd media was incorporated into expressed proteins and our subsequent optimization of AcdRS1 provide a cautionary tale to the field of genetic code expansion, as well as a potentially general solution to the problem. Explicit inclusion of the unwanted Npf in the counter-selection step yielded AcdRS2b, which had much higher selectivity toward its cognate ncAA, whereas standard rounds of positive and negative selection (against only the 20 canonical amino acids) produced the less selective AcdRS2a. Many RSs in the literature, which have never been purposefully selected for or against charging of these ncAAs, could utilize trace contaminants in batches of ncAAs synthesized in-house or bought from commercial vendors. Moreover, variations of *in vivo* availability (resulting from differential uptake, for example) may exacerbate these problems, as appears to be the case with Npf.

Permissive RSs in libraries, which provide a very efficient way of obtaining RSs for new ncAAs, are likely to be susceptible to this problem. Indeed, RSs with open binding sites that accept bulky amino acids such as Acd and Brb may be particularly prone to this difficulty. However, using such a permissive RS with an open pocket is sometimes necessary to finding an RS for an amino acid such as Acd. In some cases, RS selection for bulky ncAAs has required an initial round of selection using a more moderate sized amino acid to expand the binding pocket before selection for charging of a bulky aromatic ncAA.[16] Such RSs may be prone to misincorporation of amino acids similar to that intermediate amino acid. Here, we have seen that small sequence changes (*i.e.* Gly→Ala and Glu→Asp) can result in large increases in *in vitro* and *in vivo* selectivity for permissive RSs. Thus, we expect that the counter-selection strategy used here will be generally useful to the genetic code expansion community.

Author contributions

I. S. and L. C. S. synthesized amino acids and performed *in vivo* protein expression and MALDI MS analysis.

Z. M. H. cloned and expressed LexA and AcdRSs. R. J. B. and J. J. Po. performed AcdRS selections. C. M. D. and L. Z. M. performed AcdRS kinetic measurements. J. A. V. generated computational models. J. G. S. supervised J. A. V.; J. J. Pe. supervised. C. M. D. and L. Z. M.; R. M. K. supervised Z. M. H.; R. A. M. supervised R. J. B. and J. J. Po.; and E. J. P. supervised I. S. and L. C. S. All authors contributed to the writing of the manuscript.

Acknowledgements

This work was supported by funding from the National Science Foundation (NSF CHE-1150351 to E. J. P., NSF MCB-1518265 to R. A. M., NSF CHE-1508318 to J. G. S.), National Institutes of Health (NIH DP2-GM105444 to R. M. K.) and the Searle Scholars Program (10-SSP-214 to E. J. P.). Instruments supported by the National Science Foundation and National Institutes of Health include: LCMS/HRMS (NIH RR-023444), MALDI MS (NSF MRI-0820996), NMR (NIH RR-022442), and a stopped flow fluorometer (NSF CHE-1337449). J. G. S. acknowledges infrastructural support from the Penn Laboratory for Research on the Structure of Matter (NSF DMR 1120901) and use of the Extreme Science and Engineering Discovery Environment (XSEDE), which is supported by NSF grant ACI-1053575 under grant TG-CHE 110041. I. S. thanks the Royal Thai Foundation for fellowship support. Z. M. H. and J. A. V. thank the the NIH for funding through the Chemistry-Biology Interface Training Program (T32 GM071399). J. A. V. and J. G. S. acknowledge assistance and preliminary computational studies from Lu Gao.

Notes and references

1 D. Chin and A. R. Means, *Trends Cell Biol.*, 2000, **10**, 322–328.
2 S. W. Vetter and E. Leclerc, *Eur. J. Biochem.*, 2003, **270**, 404–414.
3 M. Butala, D. Zgur-Bertok and S. J. W. Busby, *Cell. Mol. Life Sci.*, 2009, **66**, 82–93.
4 M. J. Culyba, C. Y. Mo and R. M. Kohli, *Biochemistry*, 2015, **54**, 3573–3582.
5 H. A. Lashuel, C. R. Overk, A. Oueslati and E. Masliah, *Nat. Rev. Neurosci.*, 2013, **14**, 38–48.
6 M. G. Spillantini, M. L. Schmidt, V. M. Y. Lee, J. Q. Trojanowski, R. Jakes and M. Goedert, *Nature*, 1997, **388**, 839–840.
7 C. M. Haney, R. F. Wissner and E. J. Petersson, *Curr. Opin. Chem. Biol.*, 2015, **28**, 123–130.
8 B. N. G. Giepmans, S. R. Adams, M. H. Ellisman and R. Y. Tsien, *Science*, 2006, **312**, 217–224.
9 J. R. Lakowicz, *Principles of Fluorescence Spectroscopy*, Springer, US, 3 edn, 2006.
10 L. C. Speight, M. Samanta and E. J. Petersson, *Aust. J. Chem.*, 2014, **67**, 686–700.
11 K. Lang and J. W. Chin, *Chem. Rev.*, 2014, **114**, 4764–4806.
12 L. C. Speight, A. K. Muthusamy, J. M. Goldberg, J. B. Warner, R. F. Wissner, T. S. Willi, B. F. Woodman, R. A. Mehl and E. J. Petersson, *J. Am. Chem. Soc.*, 2013, **135**, 18806–18814.
13 A. Dumas, L. Lercher, C. D. Spicer and B. G. Davis, *Chem. Sci.*, 2015, **6**, 50–69.
14 D. Summerer, S. Chen, N. Wu, A. Deiters, J. W. Chin and P. G. Schultz, *Proc. Natl. Acad. Sci. U. S. A.*, 2006, **103**, 9785–9789.
15 J. Wang, J. Xie and P. G. Schultz, *J. Am. Chem. Soc.*, 2006, **128**, 8738–8739.
16 H. S. Lee, J. Guo, E. A. Lemke, R. D. Dimla and P. G. Schultz, *J. Am. Chem. Soc.*, 2009, **131**, 12921–12923.
17 A. Chatterjee, J. T. Guo, H. S. Lee and P. G. Schultz, *J. Am. Chem. Soc.*, 2013, **135**, 12540–12543.
18 A. H. Harkiss and A. Sutherland, *Org. Biomol. Chem.*, 2016, **14**, 8911–8921.
19 J. Luo, R. Uprety, Y. Naro, C. J. Chou, D. P. Nguyen, J. W. Chin and A. Deiters, *J. Am. Chem. Soc.*, 2014, **136**, 15551–15558.
20 A. Szymanska, K. Wegner and L. Lankiewicz, *Helv. Chim. Acta*, 2003, **86**, 3326–3331.
21 M. Taki, Y. Yamazaki, Y. Suzuki and M. Sisido, *Chem. Lett.*, 2010, **39**, 818–819.
22 H. Hamada, N. Kameshima, A. Szymanska, K. Wegner, L. Lankiewicz, H. Shinohara, M. Taki and M. Sisido, *Bioorg. Med. Chem.*, 2005, **13**, 3379–3384.
23 J. M. Goldberg, L. C. Speight, M. W. Fegley and E. J. Petersson, *J. Am. Chem. Soc.*, 2012, **134**, 6088–6091.
24 L. Wang, A. Brock, B. Herberich and P. G. Schultz, *Science*, 2001, **292**, 498–500.
25 L. Wang and P. G. Schultz, *Angew. Chem., Int. Ed.*, 2005, **44**, 34–66.
26 S. J. Miyake-Stoner, C. A. Refakis, J. T. Hammill, H. Lusic, J. L. Hazen, A. Deiters and R. A. Mehl, *Biochemistry*, 2010, **49**, 1667–1677.
27 J. C. Peeler, B. F. Woodman, S. Averick, S. J. Miyake-Stoner, A. L. Stokes, K. R. Hess, K. Matyjaszewski and R. A. Mehl, *J. Am. Chem. Soc.*, 2010, **132**, 13575–13577.
28 A. L. Stokes, S. J. Miyake-Stoner, J. C. Peeler, D. P. Nguyen, R. P. Hammer and R. A. Mehl, *Mol. Biosyst.*, 2009, **5**, 1032–1038.
29 E. Díaz, A. Ferrández, M. A. Prieto and J. L. García, *Microbiol. Mol. Biol. Rev.*, 2001, **65**, 523–569.
30 R. B. Cooley, P. A. Karplus and R. A. Mehl, *ChemBioChem*, 2014, **15**, 1810–1819.
31 M. Ibba and D. Soll, *Annu. Rev. Biochem.*, 2000, **69**, 617–650.
32 C. S. Francklyn, E. A. First, J. J. Perona and Y. M. Hou, *Methods*, 2008, **44**, 100–118.
33 S. Nehring, N. Budisa and B. Wiltschi, *PLoS One*, 2012, **7**, e31992.
34 B. J. Rauch, J. J. Porter, R. A. Mehl and J. J. Perona, *Biochemistry*, 2016, **55**, 618–628.

35 A. Rodríguez-Hernández and J. J. Perona, *Structure*, 2011, **19**, 386–396.
36 P. Belmont, J. Bosson, T. Godet and M. Tiano, *Anticancer Agents Med. Chem.*, 2007, **7**, 139–169.
37 H. Kono and J. G. Saven, *J. Mol. Biol.*, 2001, **306**, 607–628.
38 J. R. Calhoun, H. Kono, S. Lahr, W. Wang, W. F. DeGrado and J. G. Saven, *J. Mol. Biol.*, 2003, **334**, 1101–1115.
39 G. M. Bender, A. Lehmann, H. Zou, H. Cheng, H. C. Fry, D. Engel, M. J. Therien, J. K. Blasie, H. Roder, J. G. Saven and W. F. DeGrado, *J. Am. Chem. Soc.*, 2007, **129**, 10732–10740.
40 H. C. Fry, A. Lehmann, L. E. Sinks, I. Asselberghs, A. Tronin, V. Krishnan, J. K. Blasie, K. Clays, W. F. DeGrado, J. G. Saven and M. J. Therien, *J. Am. Chem. Soc.*, 2013, **135**, 13914–13926.